Half-of-Sites Binding of Orotidine 5′-Phosphate and α-D-5-Phosphorylribose 1-Diphosphate to Orotate Phosphoribosyltransferase from *Saccharomyces cerevisiae* Supports a Novel Variant of the Theorell−Chance Mechanism with Alternating Site Catalysis†

Ronald W. McClard,* Edward A. Holets,‡ Andrew L. MacKinnon,‡,§ and John F. Witte

Arthur F. Scott Laboratory of Chemistry, Reed College, Portland, Oregon 97202-8199

Received August 18, 2005; Revised Manuscript Received December 24, 2005

ABSTRACT: A ping-pong bi-bi kinetic mechanism ascribed to yeast orotate phosphoribosyltransferase (OPRTase) [Victor, J., Greenberg, L. B., and Sloan, D. L. (1979) *J. Biol. Chem. 254*, 2647−2655] has been shown to be inoperative [Witte, J. F., Tsou, R., and McClard, R. W. (1999) *Arch. Biochem. Biophys. 361*, 106−112]. Radiolabeled orotidine 5′-phosphate (OMP), generated in situ from [7-^{14}C]-orotate and α-D-5-phoshorylribose 1-diphosphate (PRPP), binds tightly enough to OPRTase (a dimer composed of identical subunits) that the complex survives gel-filtration chromatography. When a sample of OMP·OPRTase is extensively dialyzed, a 1:1 (per OPRTase dimer) complex is detected by ^{31}P NMR. Titration of the apoenzyme with OMP yields a ^{31}P NMR spectrum with peaks for both free and enzyme-bound OMP when OMP is in excess; the complex maintains an OMP/enzyme ratio of 1:1 even when OMP is in substantial excess. A red shift in the UV spectrum of the OMP·OPRTase complex was exploited to measure $K_{d(OMP)} = 0.84$ μM and to verify the 1:1 binding stoichiometry. PRPP forms a Mg^{2+}-dependent 1:1 complex with the enzyme as observed by ^{31}P NMR. Isothermal titration calorimetry (ITC) experiments revealed 1:1 stoichiometries for both OMP and Mg^{2+}-PRPP with OPRTase yielding K_d values of 0.68 and 10 μM, respectively. The binding of either 1 equiv of OMP or PRPP is mutually exclusive. ITC experiments demonstrate that the binding of OMP is largely driven by increased entropy, suggesting substantial distal disordering of the protein. Analytical gel-filtration chromatography confirms that the OMP·OPRTase complex involves the dimeric form of enzyme. The off rate for release of OMP, determined by magnetization inversion transfer, was determined to be 27 s^{-1}. This off rate is somewhat less than the k_{cat} in the biosynthetic direction (about 39 s^{-1}); thus, the release of OMP from OMP·OPRTase may not be kinetically relevant to the steady-state reaction cycle. The body of available data can be explained in terms of alternating site catalysis with either a classical Theorell−Chance mechanism or, far more likely, a novel "double Theorell−Chance" mechanism unique to alternating site catalysis, leading us to propose co-temporal binding of orotate and the release of diphosphate as well as the binding of PRPP and the release of OMP that occur via ternary complexes in alternating site fashion across the two highly cooperative subunits of the enzyme. This novel "double Theorell−Chance" mechanism yields a steady-state rate equation indistinguishable in form from the observed classical ping-pong bi-bi kinetics.

Orotate phosphoribosyltransferase (EC 2.4.2.10) (OPRTase)[1] catalyzes the condensation of orotic acid (OA) with 5-α-D-phosphorylribose 1-diphosphate (PRPP) to yield the nucleotide orotidine 5′-phosphate (OMP), which is efficiently decarboxylated by OMP decarboxylase (EC 4.1.1.23) (ODCase) to uridine 5′-phosphate (UMP), the entry nucleotide to the de novo biosynthesis of all pyrimidine nucleotides.

Yeast OPRTase, composed of two identical subunits, is a typical example of a type-I PRTase with a flexible loop over each catalytic site and a well-defined PRPP-binding domain (*1*). A clear example of such loop dynamics is that of glutamine phosphoribosylpyrophosphate amidotransferase (EC 2.4.2.14) (GPATase), in which an apparently disorganized loop that constitutes a flap closes up on bound substrate

† This work was supported by grants (to R.W.M.) from the National Institutes of Health (R15GM61317) and the Medical Research Foundation of Oregon, by a Mellon Post-Baccalaureate Fellowship (to A.L.M.), and by a grant from the National Science Foundation MRI Program (0116373) for the purchase of an NMR spectrometer.

* To whom correspondence should be addressed. Telephone: (503) 777-7218. Fax: (503) 788-6643. E-mail: mcclard@reed.edu.

‡ Both of these authors contributed equally to this work.

§ Present address: Department of Cellular and Molecular Pharmacology, University of California at San Francisco, Mission Bay Campus, San Francisco, CA 94143.

[1] Abbreviations: BMP, 1-(5′-phospho-β-D-ribofuranosyl)-barbiturate; EDTA, ethylenediamine *N*,*N*,*N*′,*N*′-tetraacetate; GPATase, glutamine phosphoribosylpyrophosphate amidotransferase (EC 2.4.2.14); ITC, isothermal titration calorimetry; MPA, methylphosphonic acid; OA, orotic acid; ODCase, OMP decarboxylase (EC 4.1.1.23); OMP, orotidine 5′-phosphate; OPRTase, orotate phosphoribosyltransferase (EC 2.4.2.10); PP_i, diphosphate; PRPP, 5-α-D-phosphorylribose 1-diphosphate; UMP, uridine 5′-phosphate.

10.1021/bi051650o CCC: $33.50
Published on Web 04/01/2006

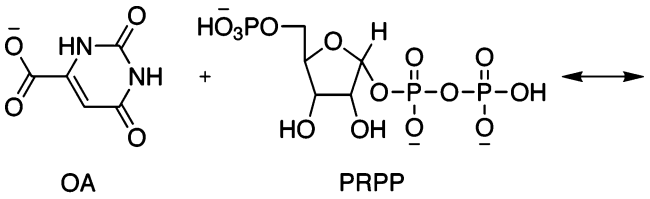

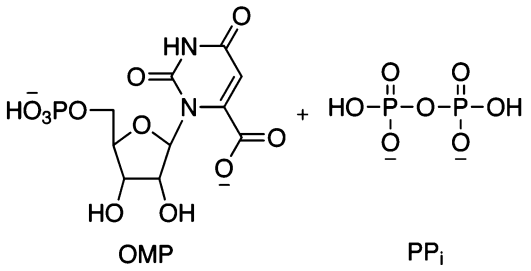

analogues and, in so doing, is accompanied by the formation of an α-helical segment (*2*).

The OPRTase from *Salmonella*, which shows a random sequential mechanism, was first crystallized as a homodimer with two bound OMP molecules and shown to possess a C2 axis of symmetry (*3*). Subsequently, a cocrystal with OA and PRPP revealed that the anomeric carbon of PRPP must swing a considerable distance (~7 Å) on the pivot point of the 5′-phosphate during catalysis (*4*). Additionally, the *Salmonella* enzyme displays a burst in the biosynthetic direction corresponding to 1.5 mol of OMP/mol of dimeric enzyme and a burst in the reverse reaction of 0.7 mol of PRPP/mol of dimer (*5*). A slow physical step during catalysis was taken to be a conformational change as evidenced by viscosity studies (*5*). The binding stoichiometries for OMP, PRPP, and OA were reported to fall somewhere between 1 and 2; however, in the presence of saturating OA, the stoichiometry is about 1 diphosphate (PP_i)/enzyme dimer (*5*). The motional dynamics of a highly conserved loop domain (the "flap" from the adjacent subunit that closes during catalysis) have been characterized by nuclear magnetic resonance (NMR) and proteolysis studies (*6*). A crystal structure of the *Escherichia coli* enzyme, with two sulfate ions bound at each of the two 5′-phoshate domains, also shows evidence of such a closing loop (*7*) and that this loop is provided by the companion subunit. There is also a considerable lack of symmetry in the sulfate-bound form, in which one of the "flaps" is well-defined in a closed position, while the other remains ill-defined and solvent-exposed.

The OPRTase from *Saccharomyces cerevisiae* is homologous to the bacterial forms, with 48.6% sequence identity and 75.5% similarity,[2] yet prior work on the yeast form led to the conclusion (*9*) that the enzyme followed an ordered sequential mechanism, in particular a ping-pong bi-bi mechanism, with PRPP binding first to the enzyme followed by the release of PP_i to yield an enzyme-bound phosphoribosyl intermediate. In turn, OA binds followed by catalysis to produce OMP, which is released last. That mechanism was consistent with the kinetic evidence (*9*), including isotope effect studies (*10*), the latter of which suggest the existence of an oxocarbenium intermediate. As required by this

[2] Determined from sequences obtained from http://www.ncbi.nlm-.nih.gov/entrez and subjected to FASTA analysis (*8*).

Scheme 1

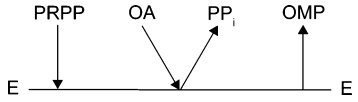

mechanism, the binding of OMP or PRPP was mutually competitive, as for the binding of OA and PP_i (*9*). In addition, when PRPP was employed as the varied substrate at fixed concentrations of OA (and vice versa), the characteristic "parallel lines" of ping-pong kinetics were observed on reciprocal plots of the kinetic data. The analogous observation was made with OMP and PP_i (*9*). The requisite half-reaction incorporations of [^{32}P]-PP_i into PRPP and [^{14}C]-OA into OMP were observed in the apparent absence of OMP or OA (*9*). However, our laboratory revisited this issue and demonstrated that purified yeast OPRTase treated with ODCase lost the ability to exchange PRPP/PP_i as measured by magnetization transfer in ^{31}P NMR (*11*). Thus, it became clear that the ping-pong bi-bi mechanism was not operative. Similar radioisotopic exchange observed for the *Salmonella* enzyme was eliminated by denaturation/dialysis/renaturation (*12*).

One kinetic mechanism that fits all of the initial rate data (*9*) and our observations (*11*) is the Theorell−Chance variant of the ordered sequential mechanism (Scheme 1), in which central ternary complex(es) has no significant lifetime with respect to the k_{cat} time scale with the condition that $K_{d(OMP)}$ is significantly lower than the $K_{m(OMP)}$. In such a circumstance, erroneous assignment to the ping-pong bi-bi mechanism might be postulated (*13*, *14*). Our observation that OMP was bound tightly enough to OPRTase to require its enzymatic removal (*11*) was in accordance with such a condition.

We demonstrate here that OMP is bound with a submicromolar K_d and, furthermore, that the enzyme binds 1 equiv of OMP (or PRPP) per dimer and thus exhibits half-of-sites reactivity. We propose an alternating site catalysis model in which the essentially co-temporal binding of OA and dissociation of PP_i, as required by the Theorell−Chance mechanism, and for OMP/PRPP as well occur across the two identical subunits in a highly cooperative fashion, known as alternating site catalysis. We also show that *all* available data are best accounted for by a novel variation of the Theorell−Chance mechanism, unique to alternating site catalysis, which we have dubbed "double Theorell−Chance".

EXPERIMENTAL PROCEDURES

General Procedures. Recombinant yeast ODCase was the generous gift of Dr. Steven Short of GlaxoSmithKline. 1-(5′-Phospho-β-D-ribofuranosyl)-barbiturate (BMP) was synthesized as described (*15*). OMP was either obtained from Sigma Chemical Co. or was synthesized by published methods (*16*, *17*). Buffers, OA as the sodium salt, PRPP, inorganic pyrophosphatase, $MgCl_2$, ethylenediamine *N*,*N*,*N*′,*N*′-tetraacetate (EDTA), D_2O, MPA, rabbit muscle creatine phosphokinase, and other reagent-grade biochemicals were also obtained from Sigma Chemical Co. [7-^{14}C] OA, 55 Ci/mol, was the product of New England Nuclear. The concentration of PRPP in working solutions was determined enzymatically as previously described (*18*) and confirmed by ^{31}P NMR using MPA as an internal standard. The concentration of the

sodium salt of OMP was determined spectrophotometrically (9.96 mM^{-1} cm^{-1} at 267 nm in H_2O) and confirmed by phosphorus analysis (*19*) and by ^{31}P NMR with MPA as an internal standard.

OPRTase from S. cerevisiae. Cloning, expression, and purification of OPRTase were as described previously (*11*). Typically, 150 mg of homogeneous enzyme was obtained per liter of culture. Routine assays (1.00 mL) were performed at 25 °C in 100 mM Tris at pH 7.8 containing 100 μM OMP, 2 mM $MgCl_2$, 4 mM PP_i, and 0.05−0.15 unit of OPRTase and were initiated, after a 2 min thermal equilibration, by the addition of the enzyme. A total of 1 IU of OPRTase activity was defined as that amount of enzyme catalyzing the conversion of 1 μmol of OMP to PRPP per minute. For all experiments, the enzyme concentration was determined kinetically, utilizing a $\Delta\epsilon_{290\ nm} = +4.40\ mM^{-1}\ cm^{-1}$ for the conversion of OMP to PRPP with saturating OMP and PP_i (routine assay) and using a specific activity of 30.0 (±3.4, $p = 0.1$, $N = 3$) IU/mg OPRTase based on gravimetric microanalysis of thoroughly dried pure protein (see below). The specific activity in the biosynthetic direction was found to be 46.5 IU/mg ($k_{cat} = 39\ s^{-1}$), using 1 mM PRPP, 0.4 mM OA, and yeast ODCase (0.4 IU) to remove OMP. Experiments to determine the kinetic constants were performed as follows: in the biosynthetic direction, OA was varied from 10 to 200 μM and PRPP was varied from 40 to 400 μM, and in the reverse direction, OMP was varied from 7.5 to 120 μM and PP_i ranged from 250 to 2200 μM. The data were fitted to appropriate models using standard Levenberg−Marquardt nonlinear regression.

Determination of OPRTase Concentrations. Freshly prepared, affinity-purified OPRTase (judged by SDS gel electrophoresis to be >99% pure) was dialyzed overnight against 1 mM Tris-HCl buffer at pH 7.8. Replicate samples (generally containing 500−2000 μg of protein in 20 μL) were placed onto aluminum disks and dried thoroughly in an Abderhalden apparatus maintained at 110 °C by refluxing toluene for 16 h under vacuum (0.01−0.05 mmHg). Replicate samples of the dialysate, also 20 μL, were treated the same way. The samples were weighed on a Cahn microbalance to ±0.1 μg, and those of the enzyme were corrected for the mass of the dialysate. Activity (IU) of a known volume (diluted as necessary) of the same sample of enzyme (prior to dialysis) was determined and used to obtain a specific activity based on the dry weight of the enzyme, determined gravimetrically as just described. This specific activity was used in all of our experiments, where it was crucial to know the concentration of active enzyme. In a similar manner, the $\epsilon^{1\%}_{280nm}$ for the apoenzyme dimer (OPRTase incubated with a small amount of ODCase and dialyzed) was found to be 3.56, equivalent to molar absorptivity = 17.5 mM^{-1} cm^{-1}.

Gel-Filtration Chromatography of a [7-^{14}C]OMP·OPRTase Complex. One reaction mixture (0.5 mL) consisted of OPRTase (20 nmol), excess sodium [7-^{14}C]-OA (40 nmol, 734 cpm/nmol), limiting PRPP (30 nmol), 1 μmol of $MgCl_2$, and pyrophosphatase (10 IU), all in 100 mM Tris at pH 7.8. The reaction mixture was incubated at 23 °C for 45 min, 15 min longer than was required for a parallel 1.00 mL reaction consisting of OPRTase (0.05 nmol), pyrophosphatase (1 IU), PRPP (100 nmol), OA (100 nmol), and Mg^{2+} (2 μmol), all in Tris buffer (100 mM, pH 7.8) to reach equilibrium, as followed spectrophotometrically. The reaction mixture was applied to a Sephadex G-25 Superfine (20−50 μm) column (1 × 46 cm) pre-equilibrated with Tris buffer (100 mM, pH 7.8) and eluted with the same buffer. Fractions (1 mL) were collected, mixed with 10 mL of Ecoscint (National Diagnostics) fluid, and subjected to liquid scintillation counting for 5 min each (Packard Model 2900 TR, 0−156 keV window). A separate reaction mixture (0.5 mL) consisted of OPRTase (6 nmol), limiting sodium [7-^{14}C]-OA (10 nmol, 8785 cpm/nmol), excess PRPP (12 nmol), 1 μmol $MgCl_2$, and pyrophosphatase (10 IU), all in 100 mM Tris at pH 7.8. The reaction was incubated at 23 °C for 45 min, again sufficient to reach completion as described above. The reaction mixture was applied to the Sephadex G-25 column, and fractions were collected and counted as described above.

Apo OPRTase. The OMP·OPRTase complex (1000−2000 IU) in 0.5−30 mL of buffer (100 mM Tris at pH 7.8 and 5 mM β-mercaptoethanol) was incubated with 0.5−4 IU of yeast ODCase. Removal of OMP from OPRTase and formation of UMP was followed either by ^{31}P NMR or UV spectroscopy. When the reaction was complete, the resulting mixture was concentrated to 0.5 mL and dialyzed at 4 °C overnight (Pierce Slide-A-Lyzers, 10 000 MW cutoff) against 1 L of 100 mM Tris at pH 7.8. After this time, an aliquot of the dialysant (10−20 μL), containing apoenzyme and a small amount of ODCase, was assayed for ODCase activity and the remaining activity, usually ca. 0.05% of the starting activity, was fully inhibited by making the solution 50−200 μM in BMP. This mixture was used in subsequent binding experiments; however, if PRPP was to be the ligand, no BMP was added to the dialyzed enzyme.

Analytical High-Performance Liquid Chromatography (HPLC) Gel Filtration. Determination of the approximate molecular weight of OPRTase was performed using a Bio-Rad Bio-Sil 250 column (7.8 × 300 mm) at a flow rate of 0.5 mL min^{-1} requiring 900−1000 psi (Rainin Dynamax SD-200 system) using isocratic 100 mM sodium phosphate buffer at pH 6.8 plus 150 mM NaCl. Proteins were detected at 256 nm. Relative retentions (retention time divided by the retention time corresponding to the void volume) of various protein standards (IgG, 158 000; rabbit muscle creatine phosphokinase, 81 000; chicken ovalbumin, 45 000; and equine myoglobin, 17 000) were plotted against the log of their respective molecular weights to yield a linear fit that allowed for an approximate estimate for the molecular weight of OPRTase in its apo (see below) and OMP-bound [as removed from the affinity column (*4*), diafiltered, and concentrated] forms.

^{31}P NMR Spectra of the OMP·OPRTase and PRPP·OPRTase Complexes. ^{31}P NMR spectra of free and enzyme-bound ligands were acquired at 162 MHz on a Bruker Avance 400 MHz spectrometer at 27 °C. For quantitative experiments, inverse-gated ^1H decoupling with a relaxation delay of 8 s was employed. Typically, 2000−10 000 scans were acquired to obtain adequate signal-to-noise ratios, and a 10 Hz window function was applied to all spectra prior to Fourier transformation. Samples (0.500 mL) in 100 mM Tris (pH 7.8) contained ~1 mM enzyme dimer, 1 mM EDTA, 10% (v/v) D_2O, 0.500 mM MPA as an internal chemical shift and integration standard, and variable amounts of OMP or Mg^{2+}-PRPP. Dialysis of 0.500 mL samples was performed in Pierce Slide-a-Lyzer dialysis cassettes (10 000 MW cutoff)

against 1 L of 100 mM Tris (pH 7.8) with 1 mM EDTA at 4 °C for 12−18 h. The measured half-life for the efflux of free OMP under these conditions was found to be 2−2.5 h.

Spectrophotometric Titration of Apo OPRTase with OMP. The spectral change accompanying the binding of OMP to apo OPRTase was quantitated in the following way. A 1.00 mL solution of 50 μM OMP in 100 mM Tris-HCl buffer (pH 7.8) was placed in one of two chambers of a notched tandem quartz cuvette (path lengths each of 0.4375 cm), and a 1.00 mL solution of 50 μM apo OPRTase (prepared as above) in the same buffer was placed in the other chamber; a spectrum was then obtained. The contents of the two chambers were mixed by inversion of the cuvette, and a second spectrum was recorded after a 5 min incubation. The first spectrum was subtracted from the second to provide a difference spectrum. The wavelength of the maximum difference was found to be 290 nm. To determine the $\Delta\epsilon$ of enzyme-bound OMP at 290 nm, an "inverse titration" (*20*) was performed in which the [OMP] was held constant at 30 μM, while the [OPRTase] was varied from 0 to 70 μM by successive dilutions with a 30 μM OMP solution in the Tris buffer. Subtractions for the absorbances of the apoenzyme and OMP were applied to yield a set of corrected data that were fitted (nonlinear regression) to eq 1.

$$\Delta A = \frac{\Delta A_{max}([E]_o - \Delta A[L]_o/\Delta A_{max})([L]_o - \Delta A[L]_o/\Delta A_{max})}{[L]_o K_d} \quad (1)$$

Here, $[E]_o$ is the concentration of included apo OPRTase, and $[L]_o$ is the fixed concentration of OMP. The fitted value ΔA_{max} was then used to obtain the molar $\Delta\epsilon$ for formation of the OMP·OPRTase complex at limiting OMP. Equation 1 can be solved for ΔA to give

$$\Delta A = \frac{\Delta\epsilon}{2}(K_d + [E]_o + [L]_o - \sqrt{K_d^2 + 2K_d[E]_o + 2K_d[L]_o + [E]_o^2 + [L]_o^2 - 2[E]_o[L]_o}) \quad (2)$$

The complementary titration was then performed at 290 nm in which [OPRTase] was fixed at 26 μM and the [OMP] was varied from 0 to 65 μM to give another set of absorbances, which were subjected to appropriate corrections for absorbances of apo OPRTase and unbound OMP, as above, and then fitted (SigmaPlot) to eq 2 to provide both the K_d of the OMP·OPRTase complex and, by floating the parameter $[E]_o$, the experimental binding stoichiometry.

Spectrophotometric Competitive Binding Titration. As a control, a difference spectrum of the PRPP·OPRTase complex was first recorded in analogy to that described above for the OMP·OPRTase complex. Into one chamber of the quartz tandem cuvette was placed 100 μM apo OPRTase and 10 mM $MgCl_2$ in buffer (100 mM Tris at pH 7.8); into the other chamber was placed 1000 μM PRPP and 10 mM $MgCl_2$ in the same buffer. A UV spectrum was recorded both before and after mixing the contents of the two chambers and a difference spectrum calculated.

For the competitive binding titration, the 1.00 mL reaction mixture at the start of the titration contained 30 μM OPRTase dimer, 30 μM OMP, 1000 μM PRPP, and 10 mM $MgCl_2$, all in 100 mM Tris buffer at pH 7.8. A titration at 290 nm (25 °C) was carried out by replacing measured volumes of the reaction mixture with an equal volume of 30 μM OPRTase, 30 μM OMP, and 10 mM $MgCl_2$ in the same buffer. To the raw absorbance measurements were applied a correction because of the absorbance of OPRTase and OMP. The resulting isotherm was fitted (nonlinear regression) to a single-site competitive binding model using $K_{d(OMP)}$ and $\Delta\epsilon_{(OMP-OPRTase)}$ as fixed parameters and floating only $K_{d(PRPP)}$.

Isothermal Titration Calorimetry (ITC) of OPRTase with OMP and PRPP. Ligand-binding studies were conducted by ITC at 25 °C with a Microcal VP-ITC instrument. Apo OPRTase was generated as described above, and BMP (80 μM) was included if OMP was the titrant. Dialysate was used to make all ligand and enzyme solutions. In cases with PRPP as the titrant, all solutions were filtered through a 0.2 μm filter (ValuePrep) prior to the determination of the concentration and titration. A typical OMP titration consisted of 29 10-μL injections of 500 μM OMP into 35 μM apo OPRTase. The time between injections ranged from 4 to 6 min and was sufficient for reaching thermal equilibrium. Baseline corrections were applied to the raw data sets. A typical PRPP titration consisted of 19 15-μL injections of 2.5 mM PRPP into 200 μM OPRTase, with both solutions containing 10 mM $MgCl_2$. The time between injections ranged from 10 to 14 min and was sufficient to attain thermal equilibrium. Baseline corrections were applied to the raw data sets, as were corrections for the binding of Mg^{2+} to PRPP. The PRPP curves were found to have a negative, nonzero upper asymptote, which was corrected with a linear addition on the order of 1 kcal/mol to the curve. Data sets were analyzed using the ORIGIN package supplied by MicroCal.

Measurement of k_{off} and k_{on} for the OMP·OPRTase Complex by ^{31}P NMR Magnetization Inversion Transfer. Samples of OPRTase (1−2 mM) and total OMP (2−4 mM) were prepared in 100 mM Tris buffer at pH 7.8 and 10% D_2O in a total of 0.500 mL in an NMR tube. Selective inversion of either the free OMP or bound OMP resonance was accomplished at 25 °C by employing the technique of Robinson et al. (*21*). The $\Delta\nu$ for the resonances is about 250 Hz at the Larmor frequency used (162 MHz), leading to an evolution delay of about 2 ms for the pulse sequence $\pi/2(x)$ − (delay, $2\Delta\nu)^{-1}$ − $\pi/2(x)$ − [chemical exchange delay] − $\pi/2(x)$ read pulse. Data were acquired using inverse-gated proton broadband decoupling and delay list cycling to minimize artifacts created by long experiment times (~24 h). Absolute peak intensities versus varied chemical-exchange delays were then measured, and unidirectional first-order flux was determined employing the method of Meyer et al. (*22*). Upon inversion of the OMP·OPRTase resonance, one can estimate the flux at the earliest linear time points (mixing delays) using eq 3 (*22*).

$$k_{flux} = \frac{-dM_{OMP}}{2M^o_{OMP}\,dt} \quad (3)$$

Because the system is at equilibrium, $k_{flux} = k_{off} = K_{d(OMP\cdot OPRTase)}k_{on}$ and it is irrelevant which peak is inverted.

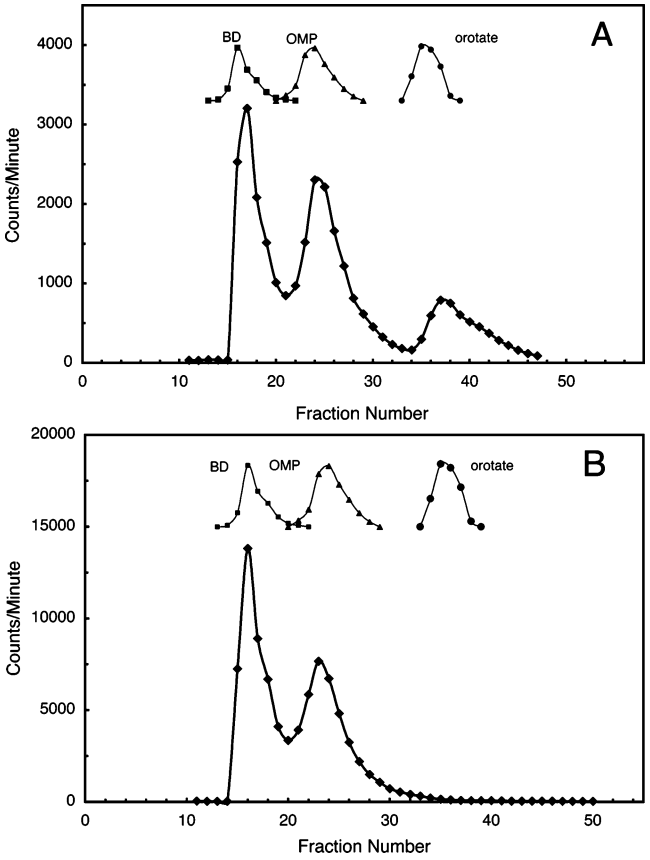

FIGURE 1: Gel-filtration chromatography of a putative OMP·OPRTase complex. (A) Elution profile of the mixture formed in the presence of an excess of OA (40 nmol, 735 cpm/nmol) over PRPP (30 nmol) and OPRTase (20 nmol) as described in the Experimental Procedures. (B) Elution profile of the reaction mixture formed with an excess of PRPP (12 nmol) over OA (10 nmol, 8785 cpm/nmol) and OPRTase (6 nmol) as described in the Experimental Procedures. The insets indicate the elution positions of blue dextran (BD), OMP, and OA as determined spectrophotometrically in a parallel experiment.

Also, it can be shown that the ratio [OMP·OPRTase]/[OMP], which was maintained ~1, has no influence on the measured k_{flux}.

RESULTS AND DISCUSSION

"Tight Binding" of OMP to OPRTase. When [7-^{14}C]-OMP was generated in situ from labeled OA, PRPP, and OPRTase and the mixture separated on a gel-filtration column, it became evident that the enzyme emerged from the column as a [7-^{14}C]OMP·OPRTase complex of unknown composition (Figure 1). We performed this experiment in an excess of OA over PRPP (Figure 1A) and with an excess of PRPP over OA (Figure 1B). We measured the total radioactivity in each of these peaks, but it was not possible to reach a conclusion as to the stoichiometry of OMP binding. It is notable that OMP (and PRPP) elutes quite early, suggesting that perhaps these species have unusually large hydrated radii. That possibility might explain why spun-column and centrifuge-ultrafiltration binding studies were unsuccessful because sufficiently clean separations of ligand and enzyme could not be achieved. Specifically, we found that 30-kD-cutoff membranes actually concentrated [7-^{14}C]-OMP rather than passing it unimpeded. It could be that this phenomenon explains why Wang et al. (*5*) observed inter-integer binding

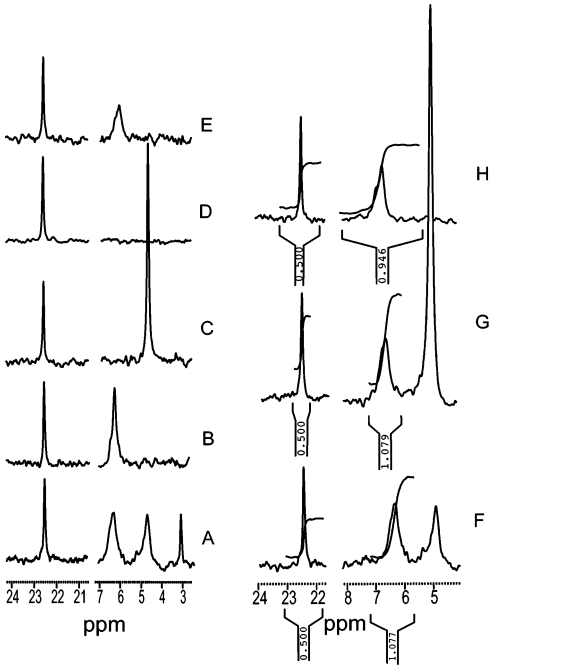

FIGURE 2: ^{31}P NMR spectra of forms of OMP in the presence of OPRTase. (Spectrum A) OPRTase dimer (1 mM) as it eluted from OMP-agarose affinity resin as described previously (*3*). The resonance at ~3 ppm is phosphate ion; the one just upfield of 5 ppm is free OMP; and the resonance at 6.4 ppm is assigned to OPRTase-bound OMP. The singlet left of the discontinuity in all spectra at 22.4 ppm is that of 0.500 mM MPA included as an internal integration standard; only noise in the large intervening region was deleted. Spectrum B shows the sample after dialysis against 2000 volumes of 100 mM Tris buffer at pH 7.8. Spectrum C shows the result of 20 min of incubation with 4 IU of ODCase; the resonance at 4.7 ppm is assigned to UMP, as evidenced by its disappearance after dialysis as described above (spectrum D). (Spectrum E) Addition of 0.7 equiv of OMP back to the sample shown in spectrum D. (Spectrum F) OPRTase (1.0 mM) in the presence of 2 equiv of OMP total. The integration of the peak assigned to OMP−OPRTase relative to MPA yields a stoichiometry of 1.08 mol of OMP/mol of OPRTase. (Spectrum G) Same as spectrum F except with 10 equiv of OMP with no change in the binding stoichiometry. (Spectrum H) Result of dialysis (against 2000 volumes of Tris buffer) of the sample shown in spectrum G.

stoichiometries for the *Salmonella* enzyme. Accordingly, we sought other approaches to quantitate binding.

Detection and Quantification of OMP·OPRTase and PRPP·OPRTase Complexes as Measured by ^{31}P NMR. The ^{31}P NMR spectrum of a concentrated solution of OPRTase contained three peaks, which were ascribed to free OMP, OMP·OPRTase, and P_i (Figure 2A). The peaks assigned to free OMP (5.0 ppm) and P_i (3.1 ppm) were identified by an admixture of authentic OMP and P_i with the sample. Overnight dialysis of the sample resulted in the disappearance of the P_i and free OMP peaks but retention of the peak at 6.4 ppm (Figure 2B), which was unambiguously assigned to an OMP·OPRTase complex. Confirmation of this assignment was achieved by incubation of the sample with several units of yeast ODCase (to convert putative OMP to UMP), which resulted in the appearance of a new peak at 5.0 ppm, identical in chemical shift with that of UMP, along with the disappearance of the peak at 6.4 ppm (parts B and C of Figure 2). A second dialysis removed all phosphorus-containing compounds from the sample (spectrum D), consistent with the negligible binding affinity of UMP for OPRTase (*23*). Finally, re-addition of a substoichiometric

amount of authentic OMP to the now apoenzyme resulted in the reappearance of the peak at 6.4 ppm (spectrum E). It should be noted that >99% of the ODCase added to remove OMP from OPRTase became inactivated during dialysis presumably because of the lack of a thiol reagent to stablilize the ODCase (*23*).

To determine the concentrations of the various phosphorus-containing species, we included MPA as an internal standard because its chemical shift (22.4 ppm) was well-separated from that of free OMP and the complex. Thus, in the presence of a slight excess of OMP over the enzyme, we found that 1.08 mol of OMP was bound per 1 mol of enyzme dimer (Figure 2F) and that this value did not change even when the concentration of OMP in the sample was increased to a 5-fold molar excess over the enzyme (Figure 2G) nor did a new peak corresponding to occupation of a second site appear. Additionally, the 1:1 binding stoichiometry did not change significantly upon overnight dialysis of the complex (Figure 2H), where the observed stoichiometry was 0.95 mol of OMP/mol of OPRTase, again in accordance with the prediction (*11*) that, upon dialysis, significant binding of the ligand would be observed even in the case of a $K_d \sim 10^{-6}$ M (see below). Replicate experiments (not shown) confirmed the observed stoichiometry of the complex, yielding values of 1.07 and 0.97 mol of OMP/mol of OPRTase. These data indicate strict half-of-sites binding of OMP by the OPRTase dimer.

We found that enzyme-bound and free forms of PRPP could also be distinguished in the ^{31}P NMR. The titration of apo OPRTase with Mg^{2+}-PRPP (parts A−D of Figure 3) allowed for the unambiguous assignment of resonances to both species, and Mg^{2+} was required for binding. The peak intensities for bound and free PRPP indicated that approximately 1 mol is bound, while 2 mol remains unbound (Figure 3C) after a total of 3 equiv of PRPP was added to this sample of the apoenzyme. We next determined precisely the PRPP-binding stoichiometry by integration of the bound (−11.8 ppm) and free α (−10.8 ppm) phosphorus resonances relative to that of the 0.500 mM MPA internal standard to yield a value of 0.91 (Figure 3E). This value did not change significantly (0.93) upon extensive dialysis of the PRPP·OPRTase complex (Figure 3F).

Binding of OMP to OPRTase as Measured by UV Difference Spectrophotometry. While apo OPRTase generated by incubation of the complex with ODCase alone was deemed adequate for the NMR studies because of the fortuitous instability of the latter enzyme, in subsequent binding experiments between apoenzyme and OMP, the potent inhibitor BMP (*15*) was included. We determined that BMP did not inhibit OPRTase, and thus, for equilibrium binding studies, the [BMP] was held at a value sufficient to completely inhibit residual ODCase activity.

The binding of OMP to apo OPRTase was accompanied by a red shift in the UV spectrum of a mixture of apo OPRTase and OMP relative to the two components unmixed in a tandem cell (Figure 4). The difference peak at 290 nm was selected because background absorbance contributed by the enzyme, OMP, and BMP was minimized. To determine the molar $\Delta\epsilon$ for formation of OPRTase-bound OMP versus the unmixed components, we first performed an "inverse titration" (*20*), in which the [OMP] was held constant and the [OPRTase] was varied to a level ≫[OMP] to saturate

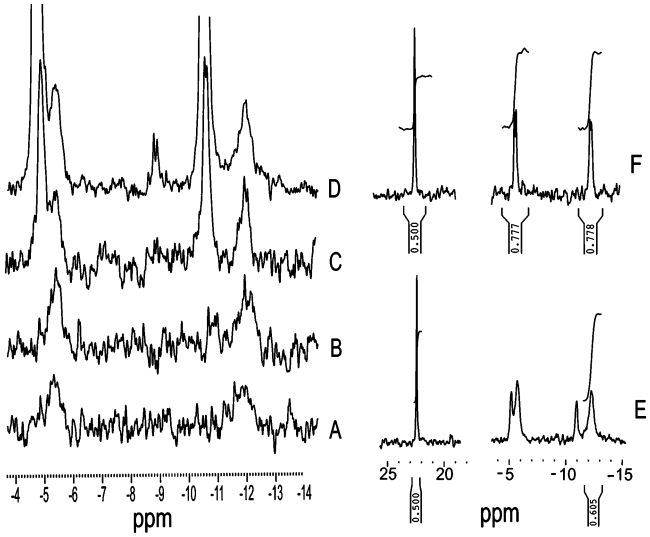

FIGURE 3: ^{31}P NMR spectra of forms of PRPP in the presence of OPRTase. Spectra A−D show resonances in the anhydride region obtained during titration of apo OPRTase with PRPP. (Spectrum A) Apo OPRTase (0.99 mM), prepared as described in the Experimental Procedures, in the presence of 14 mM $MgCl_2$, 0.53 mM PRPP, and 1 mM EDTA in 100 mM Tris buffer at pH 7.8. The ratio of [PRPP]/OPRTase was varied as 0.53 (spectrum A), 1.26 (spectrum B), 3.07 (spectrum C), and 9.8 (spectrum D). The resonances for OPRTase-bound PRPP come at −12.0 and −5.3 ppm for the α and β phosphorus atoms, respectively, while those of free PRPP come at −10.7 and −5.0 ppm. (Spectrum E) OPRTase (0.66 mM) in the presence of 1.5 equiv of PRPP, 14 mM $MgCl_2$, and 0.500 mM MPA in Tris buffer. Integration of the peak assigned to the PRPP−OPRTase complex yields a stoichiometry of 0.91 mol of PRPP/mol of OPRTase. (Spectrum F) Result of the saturating solution of apo OPRTase with 7 mM PRPP and 14 mM $MgCl_2$, followed by two cycles of dialysis (each cycle with 2000 volumes of 100 mM Tris at pH 7.8). After reintroduction of MPA at 0.500 mM and remeasurement of the [OPRTase] (0.84 mM), integration of the α or β resonance results in a binding stoichiometry of 0.93 mol of PRPP/mol of OPRTase.

the OMP with the enzyme. The data (Figure 5A) from this titration provided an excellent fit to eq 1 for a process A + B → A·B, where $[A]_o \geq [B]_o$, to yield a $\Delta\epsilon$ of 5.83 mM^{-1} cm^{-1} at 290 nm and a $K_{d(OMP)}$ of 0.95 μM assuming a 1:1 binding stoichiometry. We then performed the titration where OMP was allowed to saturate apo OPRTase (Figure 5B), and the data were fitted to eq 2 with the [OPRTase sites], *n*, and $K_{d(OMP)}$ as floating parameters. Nonlinear regression analysis yielded $n = 0.96$ and $K_{d(OMP)} = 0.84$ μM, confirming that there is one "tightly bound" OMP molecule/dimeric OPRTase molecule.

Binding of OMP and PRPP to OPRTase as Measured by ITC. The titration of apo OPRTase with OMP at 25 °C was found to produce a moderately exothermic event (Figure 6) with a sinusoidal shape characteristic of single-site binding. The heat effects associated with the dilution of OPRTase, OMP, or BMP were measured and found to be negligible. The data, when fitted to the single-site model, yielded the following stoichiometric and thermodynamic constants ($N = 4$, $p = 0.10$): 1.1 ± 0.1 mol of OMP bound/mol of OPRTase dimer, $K_d = 0.68$ (±0.31) μM, $\Delta H° = -2.4 \pm 0.4$ kcal/mol, and $\Delta S° = +20.5 \pm 2.0$ cal mol^{-1} K^{-1}. The 1:1 binding stoichiometry is in agreement with the ^{31}P NMR and UV spectroscopic experiments, again indicating half-of-sites binding of OMP to OPRTase, and the K_d is in excellent agreement with that obtained by UV spectroscopic

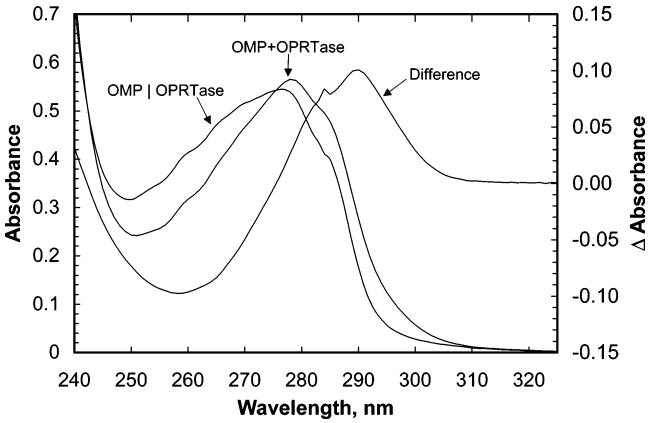

FIGURE 4: Detection of the OMP·OPRTase complex by UV difference spectroscopy. The difference spectrum of the OMP·OPRTase complex was measured in the following way. A 1.00 mL solution of 50 μM OMP in 100 mM Tris-HCl buffer (pH 7.8) was placed in one of two chambers of a notched tandem quartz cuvette (path lengths each of 0.4375 cm), and a separate 1.00 mL solution of 50 μM apo OPRTase (prepared as above) in the same buffer was placed in the other chamber. The resulting spectrum is shown as "OMP | OPRTase". Then, the contents of the two chambers were mixed by inversion of the cuvette, and a second spectrum was recorded after a 5 min incubation ("OMP + OPRTase"). The spectrum of the sum of individual components was subtracted from that of the mixture to provide the difference spectrum ("difference"). The wavelength of the maximum difference occurs at 290 nm.

titration. It is important to note that the binding of 1 mol of OMP to the apoenzyme is driven mainly by the entropic contribution ($-T\Delta S° = -6.1$ kcal/mol). This large increase in disorder must be due to the release of water and/or small ions (either from OMP or OPRTase) and/or to a substantial disordering of the protein distal to the binding site, perhaps at the adjoining vacant subunit. The latter intriguing explanation could be at the heart of the strong negative cooperativity evidenced by the observed binding stoichiometry.

The titration of PRPP into apo OPRTase at 25 °C was found to produce heat effects from two simultaneous binding processes, one exothermic and one endothermic. The heat effects associated with the dilution of OPRTase and PRPP were measured and found to be negligible. Because the binding of Mg^{2+} to PP_i is known to be endothermic (*24*), it was hypothesized that the endothermic event was the binding of Mg^{2+} to PRPP. Indeed, titrations of PRPP (no Mg^{2+}) into Mg^{2+} gave a strong endothermic binding isotherm with a curve characteristic of a two-sequential-site binding model. When the data for the titration of PRPP into the buffer (in the presence of Mg^{2+}) were subtracted from the titration of PRPP into apo OPRTase (Figure 7, top), a moderately exothermic binding isotherm resulted (Figure 7, bottom), with the characteristic sinusoidal shape of a single-site binding model. This isotherm typically had its upper asymptote at about -1 kcal/mol, which resulted from an unidentified heat of dilution. This was corrected for by the linear addition of heat sufficient to move the asymptote to 0 kcal/mol. The corrected data, when fit to the single-site model, yielded the following averaged stoichiometric and thermodynamic constants ($N = 3$, $p = 0.10$): 1.0 ± 0.2 mol of PRPP/mol of OPRTase dimer, $K_d = 10$ (± 3) μM, $\Delta H° = -4.5 \pm 0.5$ kcal/mol, and $\Delta S°$ of 7.8 ± 1.2 cal mol^{-1} K^{-1}. The binding stoichiometry is in agreement with the value obtained by ^{31}P NMR, and the K_d is consistent with the observation (^{31}P

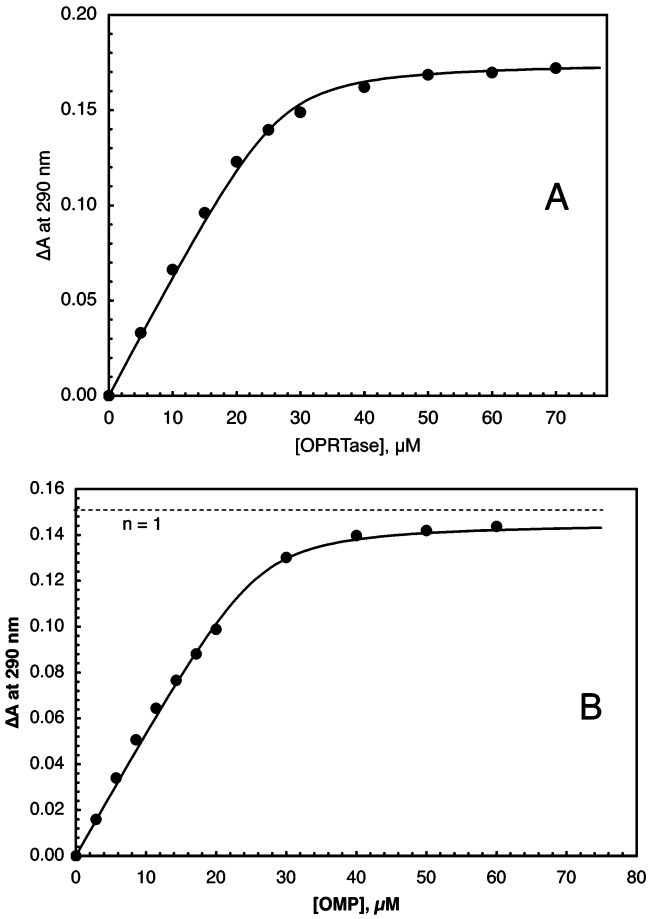

FIGURE 5: UV spectrophotometric titration of apo OPRTase with OMP to determine binding stoichiometry and K_d. (A) "Inverse titration" of 30 μM OMP with apo OPRTase performed at 290 nm and 25 °C. The molar $\Delta\epsilon$ for bound OMP (5.83 mM^{-1} cm^{-1}) was found by subtracting absorbances because of OMP and apo OPRTase from the raw absorbances and fitting (SigmaPlot) the resulting isotherm to eq 2 (—). Titration of apo OPRTase was then performed (B) by saturating 26 μM apo OPRTase with OMP, and after correction of the raw absorbances, the resulting isotherm was fitted (SigmaPlot) to eq 3 (—) yielding $n = 0.96$ (± 0.03) mol of OMP/mol of OPRTase dimer and $K_{d(OMP)} = 0.84$ (± 0.17) μM (uncertainties at $p = 0.1$).

NMR) that nearly 1 mol of PRPP remains attached to OPRTase after dialysis. Half-of-sites binding of PRPP to OPRTase is accordingly inferred from these results. In the case of PRPP, in contrast to OMP, binding is due slightly more to enthalpic rather than entropic contributions. Nevertheless, the positive $\Delta S°$ still suggests that significant distal disordering of the protein may cause the observed negative cooperativity.

Binding Competition between OMP and PRPP. There was no difference between the spectrum of a mixture containing apo OPRTase and saturating Mg^{2+}-PRPP and the spectrum of the two components separated in a tandem cuvette. This allowed us to determine $K_{d(PRPP)}$ by UV spectroscopic competitive binding titration, wherein Mg^{2+}-PRPP competes with OMP for OPRTase sites. The result of one such titration (Figure 8) yielded $K_{d(PRPP)} = 8.4$ μM, in excellent agreement with the results obtained by ITC (Figure 7), and also indicates that a ternary complex with both OMP and Mg^{2+}-PRPP bound to apo OPRTase does not form.

Measurement of the On- and Off Rates for the OPRTase−OMP Complex. Attempts to measure the k_{off} of the OMP·

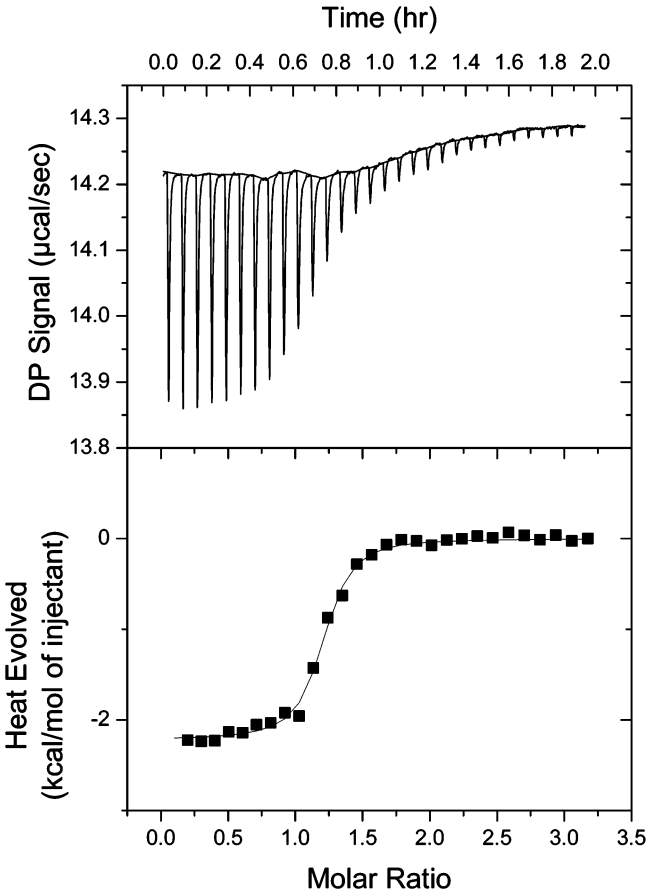

FIGURE 6: ITC of binding of OMP to apo OPRTase. The example uncorrected the differential power (DP) data (upper panel) and isotherm (lower panel) for binding of OMP to apo OPRTase. The titration employed 29 10-μL injections of 522 μM OMP into 37.5 μM apo OPRTase in the presence of 80 μM BMP at 25 °C and pH 7.8. For this titration, the fitted parameters (single-site model) were $n = 1.17$ mol of OMP/mol of OPRTase dimer, $K_d = 3.55 \times 10^{-7}$ M, $\Delta H° = -2.219$ kcal/mol OMP, and $\Delta S° = 22.1$ cal mol^{-1} K^{-1}.

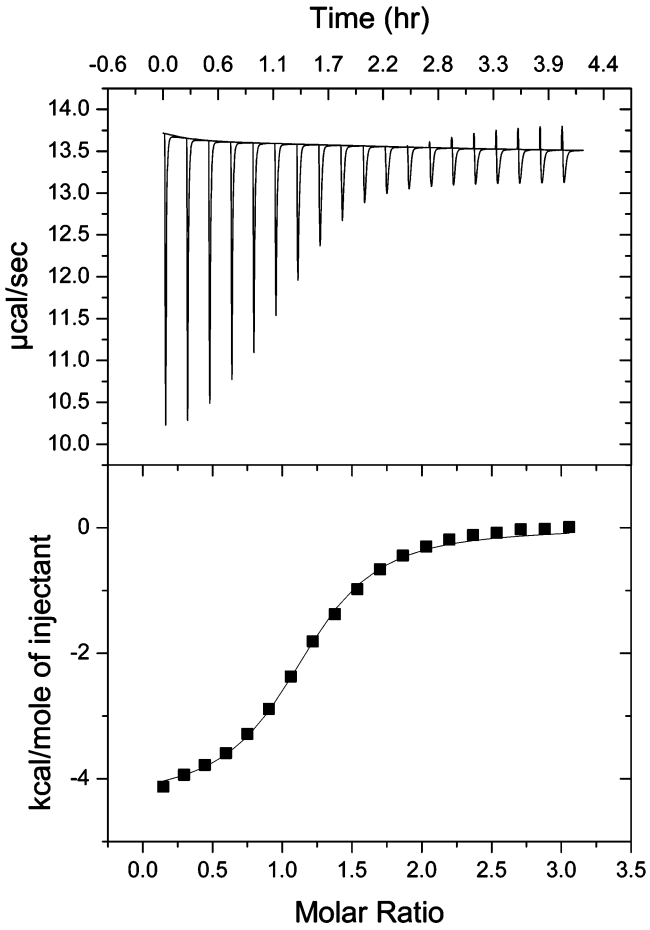

FIGURE 7: ITC of binding of Mg^{2+}-PRPP to apo OPRTase. The example uncorrected the DP data (upper panel) and isotherm (lower panel) for binding of PRPP to apo OPRTase. The titration employed 19 15-μL injections of 2.45 mM PRPP into 177 μM apo OPRTase in the presence of 10 mM Mg^{2+} at 25 °C and pH 7.8. For this titration, the fitted parameters (single-site model) were $n = 1.13$ mol of PRPP/mol of OPRTase dimer, $K_d = 1.25 \times 10^{-5}$ M, $\Delta H° = -4.322$ kcal/mol PRPP, and $\Delta S° = 7.95$ cal mol^{-1} K^{-1}.

OPRTase complex using the dialysis method of Kline and Schramm (*25*) were unsuccessful (data not shown) because one cannot measure a rate that is comparable to or faster than the rate of dialysis out of the membrane. We found that the fastest device available, to our knowledge (Slide-A-Lyzer, Pierce Chemical Co.), specifies a rate of dialysis for $Na^+ \leq 6 \times 10^{-4}$ s^{-1}. We found that for OMP this rate was nearly an order of magnitude lower at about 8×10^{-5} s^{-1} at 25 °C (data not shown). Consequently, we turned to ^{31}P NMR to measure the off rate, utilizing magnetization transfer methodology because the equilibrium exchange between free and bound forms of OMP lies in the slow-exchange domain, as evidenced by the difference in chemical shifts in the ^{31}P NMR (Figure 2). The threshold exchange rate can be taken to be $\approx$250 s^{-1}, and the existence of the two well-resolved resonances indicates that the rate is well below that. We employed the "δ-ordered" inversion technique of Robinson et al. (*21*) to invert the resonance of the OMP·OPRTase complex and observed the transfer of magnetization into the unbound OMP resonance as a function of time (see Figure 9). Only those peak intensity data acquired during the first few milliseconds of exchange time, as described by Meyer et al. (*22*), were employed to obtain $k_{off} = 27$ (± 5, $p = 0.1$, $N = 3$) s^{-1} at 25 °C. Given the average K_d for the OMP·OPRTase obtained from our UV difference and ITC methods, we calculated that $k_{on} = 3.6 \times 10^7$ M^{-1} s^{-1}. It should be noted that the k_{off} measured in this way is slightly (yet significantly) below the turnover rate of the enzyme at 25 °C (39 s^{-1}), and thus, one could infer that the dissociation of OMP from the OMP·OPRTase complex may not represent an actual process in the steady-state reaction cycle.

Postulated Kinetic Mechanisms for Yeast OPRTase. The correct kinetic mechanism for yeast OPRTase must take into account the following: (1) binding of OA and PP_i are strictly competitive, as are the binding of OMP and PRPP; (2) the kinetics for varied concentrations of the substrate pairs (PRPP/OA and OMP/PP_i) show the classical "parallel lines", heretofore uniquely characteristic of a ping-pong bi-bi mechanism; (3) there is strict half-of-sites binding of OMP and PRPP; (4) single-site binding of PRPP or OMP is mutually exclusive; and (5) the rate of release of OMP from the binary OMP·OPRTase complex (27 s^{-1}) is somewhat slower than k_{cat} in the biosynthetic direction (39 s^{-1}), thus calling into question the role of such a species as a participant in the catalytic cycle. The only classical mechanism that *might* satisfy these observations is a Theorell−Chance mechanism, with the proviso that the observed parallel lines (*2*) were the result of the $K_{d(OMP)}$ being significantly lower

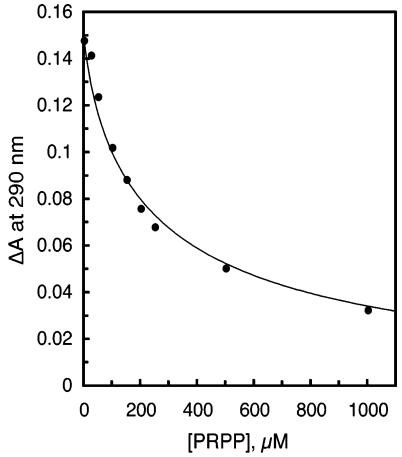

FIGURE 8: UV spectrophotometric competitive binding titration. The [OPRTase] and [OMP] were held constant at 30 μM; $MgCl_2$ was held at 10 mM; and the [PRPP] was varied. The titration was carried out by replacing measured volumes of the 1.00 mL reaction and with an equal volume of a stock solution containing 30 μM OPRTase, 30 μM OMP, and 10 mM $MgCl_2$, thereby diluting the [PRPP]. The raw absorbance measurements were corrected for absorbance because of OPRTase and OMP, and the resulting isotherm was fitted (nonlinear regression) to a single-site competitive model yielding $K_{d(PRPP)} = 8.4$ μM ($\pm$0.7, SD). During fitting, the $K_{d(OMP)}$ and $\Delta\epsilon_{(OMP-OPRTase)}$ were fixed at 0.84 μM and 5.83 mM^{-1} cm^{-1}, respectively, as determined in Figure 5.

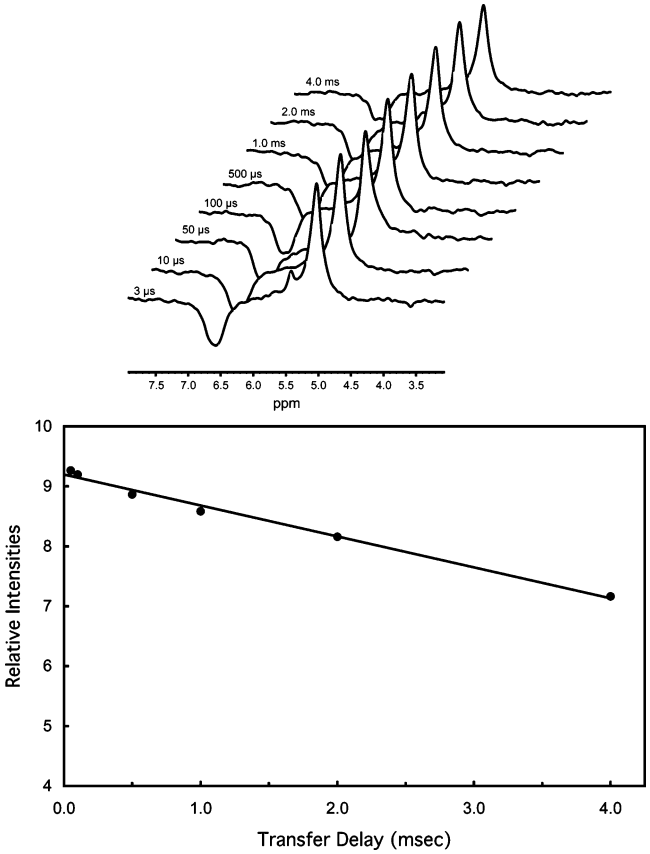

FIGURE 9: Magnetization inversion transfer experiment to determine k_{off} for the OMP·OPRTase complex. A sample of 1.96 mM OMP·OPRTase with 3.1 mM free OMP plus 4.9 mM MPA (internal standard) in 100 mM Tris-HCl buffer at pH 7.8 containing 0.05% NaN_3 and 10% D_2O at 25 °C was subjected to ^{31}P NMR inversion transfer pulse sequence as described in the Experimental Procedures. Above is the stack plot showing the inverted OMP·OPRTase resonance at 6.6 ppm and the uninverted OMP resonance at 5.1 ppm (the small peak at 5.5 ppm is due to a breakdown product of OMP). The delay times for each spectrum are shown. Below shows the intensity of the OMP resonance as a function of transfer delay along with the linear least-squares fit of the data. Use of eq 3 for a set of three replicate determinations yielded $k_{off} = 27$ ($\pm$5, $p = 0.1$, $N = 3$) s^{-1}.

than the $K_{m(OMP)}$ (with an analogous argument for PRPP). However, the requisite effectively co-temporal binding of OA and departure of PP_i, two species that are structurally unrelated, is unlikely to occur on a single catalytic site, particularly if one takes into account that type-I PRTases require an opening and closing of an active-site "flap" during catalysis (*1*, *2*, *6*, *7*). Because the release of OMP from a binary complex with the dimeric enzyme may not be a kinetically competent process, it might be that some other event effects its release.

The existence of half-of-sites reactivity in *Saccharomyces* OPRTase suggests that this on/off process occurs in toggle-like fashion across the two subunits of the enzyme as has been suggested by Scapin et al. (*4*) for *Salmonella* OPRTase. Thus, one could imagine a process like that in Scheme 2 (the rotation about the C2 axis is not a kinetic event but helps to simplify the scheme), which shows one of four possible variations to which we will refer as a *quasi-classical* Theorell−Chance mechanism, because the free enzyme is not part of the catalytic cycle. The other three variations can be generated by changing the order of catalytic events and the binding/leaving order of the substrates. The scheme shows one of two possibilities, where OMP is only bound in quaternary complexes within the catalytic cycle; one of two homologous mechanisms in which PRPP is found only within quaternary complexes is shown as Scheme 3. Presumably, the displacement, through space, of PP_i by OA (Scheme 2) or OMP by PRPP (Scheme 3) occurs at a rate such that any intermediate with all four substrates bound has a very short lifetime on the k_{cat} time scale. Because of the 2-fold axis of symmetry in the *Salmonella* enzyme (*3*, *4*) and the *Saccharomyces* enzyme,[3] the ternary complex (E·PRPP·OA) would be the same form at the start and finish of the cycle, explaining the competitive binding observed for OA versus

Scheme 2

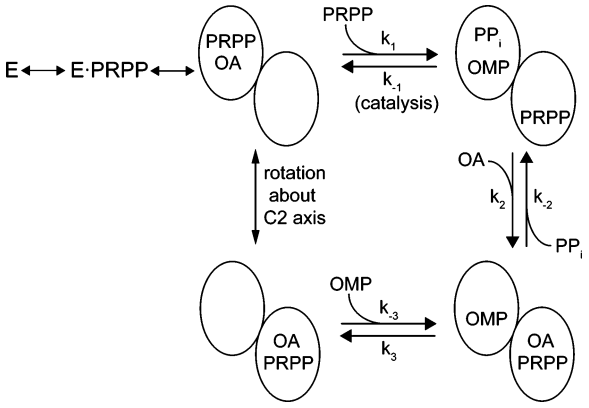

PP_i and OMP versus PRPP.[4] Dissociation of OA by PP_i (or the reverse) and dissociation of PRPP (or the reverse) would then occur across the two subunits of the enzyme in a highly cooperative fashion, reminiscent of the binding change mechanism of F1-ATP synthase (*26*).

[3] T. D. Hurley, personal communication.

Scheme 3

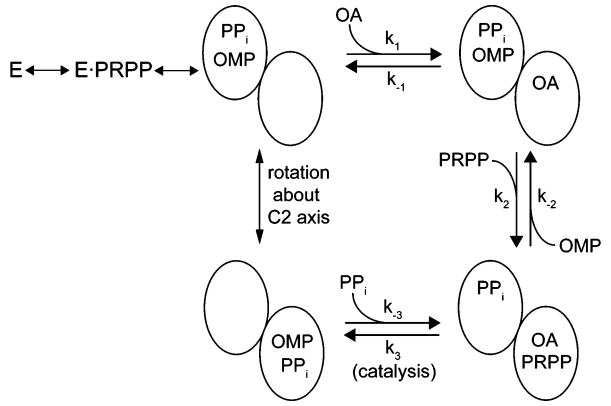

We repeated the kinetic studies of Victor et al. (*9*) and observed, in addition to the product inhibition patterns, the same set of parallel lines in double-reciprocal plots of two-substrate initial velocity measurements (plots not shown). Equations 4a and 4b are the standard forms in terms of K_m and K_i values for an ordered sequential bi-bi mechanism

$$v_f = \frac{V_f[\mathrm{PRPP}][\mathrm{OA}]}{K_{i(\mathrm{PRPP})}K_{m(\mathrm{OA})} + K_{m(\mathrm{PRPP})}[\mathrm{OA}] + K_{m(\mathrm{OA})}[\mathrm{PRPP}] + [\mathrm{PRPP}][\mathrm{OA}]} \quad (4a)$$

$$v_r = \frac{V_r[\mathrm{OMP}][\mathrm{PP_i}]}{K_{i(\mathrm{OMP})}K_{m(\mathrm{PPi})} + K_{m(\mathrm{OMP})}[\mathrm{PP_i}] + K_{m(\mathrm{PPi})}[\mathrm{OMP}] + [\mathrm{OMP}][\mathrm{PP_i}]} \quad (4b)$$

When the King−Altman method (*27*) is applied to the quasi-classical Theorell−Chance mechanism in Scheme 2, one obtains the initial rate equations for the forward and reverse reactions

$$v_f = \frac{k_1k_2k_3[\mathrm{PRPP}][\mathrm{OA}][\mathrm{E}]_t}{k_1k_3[\mathrm{PRPP}] + k_2k_3[\mathrm{OA}] + k_1k_2[\mathrm{PRPP}][\mathrm{OA}] + k_{-1}k_3} \quad (5a)$$

$$v_f = \frac{k_{-1}k_{-2}k_{-3}[\mathrm{OMP}][\mathrm{PP_i}][\mathrm{E}]_t}{k_{-1}k_{-3}[\mathrm{OMP}] + k_{-1}k_{-2}[\mathrm{PP_i}] + k_{-2}k_{-3}[\mathrm{OMP}][\mathrm{PP_i}] + k_{-1}k_3} \quad (5b)$$

By nonlinear regression analysis of our rate data to eqs 4a and 4b, we obtained the K_m values by fitting the data using K_i values calculated from the appropriate ratios of their microscopic rate constants (Table 1). Using appropriate slopes and intercepts (weighted linear regression) from double-reciprocal plots and eqs 5a and 5b, all of the microscopic rate constants were extracted and displayed in Table 1. The same set of operations were performed for the alternate mechanism shown in Scheme 3. What is most notable is that the K_m values are not sufficiently larger than their corresponding K_d values, as would be required for any compulsory ordered bi-bi mechanism, where "parallel lines" would be observed. In the case where PRPP directly displaces OMP (Scheme 3), the analysis "blows up" as the $K_{i(PPi)}$ is found to be greater than its companion K_m, which is mathematically incompatible with the observation of "parallel lines". The mechanism depicted in Scheme 2 (and its counterpart, in which one begins with $\exists E^{PRPP}_{orotate}$ and catalysis occurs in step 1) requires that OMP and PRPP be simultaneously bound to the enzyme, which does not occur, and both of these mechanisms can be eliminated on these grounds as well. Thus, the quasi-classical mechanisms of Schemes 2 and 3 appear to be highly improbable.

It occurred to us that OPRTase could effect catalysis in another rather novel manner. In this model, depicted in Scheme 4, the free enzyme is again not part of the steady-state cycle and effectively simultaneous binding/release of PRPP/OMP and OA/PP_i pairs is orchestrated across the two subunits in a "double Theorell−Chance" mechanism. It can be shown that this kinetic mechanism is completely consistent with all data reported for yeast OPRTase without condition, in particular, no restraints on the relative magnitudes of K_m and K_d. When the King−Altman method is applied to the "double Theorell−Chance" mechanism, one obtains the initial rate equation for the biosynthetic reaction and its counterpart in the reverse direction

$$v_f = \frac{k_3[\mathrm{E}]_t[\mathrm{OA}]_o[\mathrm{PRPP}]_o}{\frac{k_3[\mathrm{PRPP}]_o}{k_1} + \frac{(k_2 + k_{-2})[\mathrm{OA}]_o}{k_2} + \frac{k_3[\mathrm{OA}]_o[\mathrm{PRPP}]_o}{k_2}} \quad (6a)$$

$$v_r = \frac{k_{-1}[\mathrm{E}]_t[\mathrm{PP_i}]_o[\mathrm{OMP}]_o}{\frac{k_{-1}[\mathrm{PP_i}]_o}{k_{-3}} + \frac{(k_2 + k_{-2})[\mathrm{OMP}]_o}{k_{-2}} + \frac{k_{-1}[\mathrm{PP_i}]_o[\mathrm{OMP}]_o}{k_{-2}}} \quad (6b)$$

Note that eqs 6a and 6b lack a "constant term" in the denominator and thus are of the form that one expects for the ping-pong bi-bi mechanism. Equations 6a and 6b can then be readily inverted to yield eqs 7a and 7b

$$\frac{[\mathrm{E}]_t}{v_f} = \frac{k_2 + k_{-2}}{k_2k_3}\frac{1}{[\mathrm{PRPP}]_o} + \frac{1}{k_1[\mathrm{OA}]_o} + \frac{1}{k_2} \quad (7a)$$

$$\frac{[\mathrm{E}]_t}{v_r} = \frac{k_2 + k_{-2}}{k_{-1}k_{-2}}\frac{1}{[\mathrm{PP_i}]_o} + \frac{1}{k_{-3}[\mathrm{OMP}]_o} + \frac{1}{k_{-2}} \quad (7b)$$

In this form, it is clear that the slope of a double-reciprocal plot, with either PRPP or OA as the nominal varied substrate, is a constant and remains constant as the concentration of the other substrate is varied (and likewise for the reverse direction). Thus, this "double Theorell−Chance" mechanism predicts that classical ping-pong kinetics, as were reported by Victor et al. (*9*) and by us, will be observed without any constraints on the relative magnitudes of $K_{d(OMP)}$ versus $K_{m(OMP)}$ or $K_{d(PRPP)}$ versus $K_{m(PRPP)}$ and half-reaction exchanges become moot. In analogy to the analysis of the quasi-classical Theorell−Chance mechanism, all of the

[4] It is straightforward to prove that symmetry is not an absolute requirement by deriving the rate equation in which the E·OA·PRPP complex is isomeric to E′·OA·PRPP (or for any other similar pair). The King−Altman diagram, hexagon, instead of triangle, yields precisely the same form of equation with more kinetic constants.

Table 1: Summary of Kinetic Parameters for OPRTase

	T−C (Scheme 2)[a]	T−C (Scheme 3)[b]	"double T−C" (Scheme 4)[c]
k_1	1.8 (0.7) × 10^6 M^{-1} s^{-1}	2.6 (0.6) × 10^6 M^{-1} s^{-1}	2.6 (0.6) × 10^6 M^{-1} s^{-1}
k_{-1}	25 (1) s^{-1}	25 (1) s^{-1}	1.4 (0.4) × 10^6 M^{-1} s^{-1}
k_2	2.6 (0.6) × 10^6 M^{-1} s^{-1}	1.8 (0.7) × 10^6 M^{-1} s^{-1}	33 (6) s^{-1}
k_{-2}	0.6 (0.3) × 10^6 M^{-1} s^{-1}	1.3 (0.4) × 10^7 M^{-1} s^{-1}	25 (1) s^{-1}
k_3	38 (8) s^{-1}	38 (8) s^{-1}	3.1 (0.9) × 10^6 M^{-1} s^{-1}
k_{-3}	1.3 (0.4) × 10^7 M^{-1} s^{-1}	0.6 (0.3) × 10^6 M^{-1} s^{-1}	1.3 (0.4) × 10^7 M^{-1} s^{-1}
$K_{i(PRPP)}$ (k_{-1}/k_1)	13.9 μM		
$K_{i(OMP)}$ (k_3/k_{-3})	2.9 μM		
$K_{i(OA)}$ (k_{-1}/k_1)		9.6 μM	
$K_{i(PPi)}$ (k_3/k_{-3})		63 μM	
$K_{m(PRPP)}$ (μM)	20 (4)[d]	16 (2)[e]	18 (3)[f]
$K_{m(OA)}$ (μM)	15 (2)[d]	21 (4)[e]	20 (2)[f]
$K_{m(PPi)}$ (μM)	38 (6)[g]	ND[h]	47 (7)[f]
$K_{m(OMP)}$ (μM)	1.5 (0.2)[g]	ND[h]	2.1 (0.2)[f]

[a] For the quasi-classical Theorell−Chance mechanism shown in Scheme 2. All uncertainties in parentheses in this table are standard errors of the mean. [b] For the quasi-classical Theorell−Chance mechanism shown in Scheme 3. [c] For the double Theorell−Chance mechanism in Scheme 4. [d] Values are determined by nonlinear regression fitting by setting $K_{i(PRPP)}$ to its appropriate value from the table. [e] Values are determined by nonlinear regression fitting by setting $K_{i(OA)}$ to its appropriate value from the table. [f] Values are obtained from nonlinear regression analysis of the initial rate data. [g] Values are determined by nonlinear regression fitting by setting $K_{i(OMP)}$ to its appropriate value from the table. [h] Fitting of this model is unsuccessful because of the fact that $K_{m(PPi)} < K_{d(PPi)}$, which is mathematically inconsistent with the observation of (near) "parallel lines".

Scheme 4

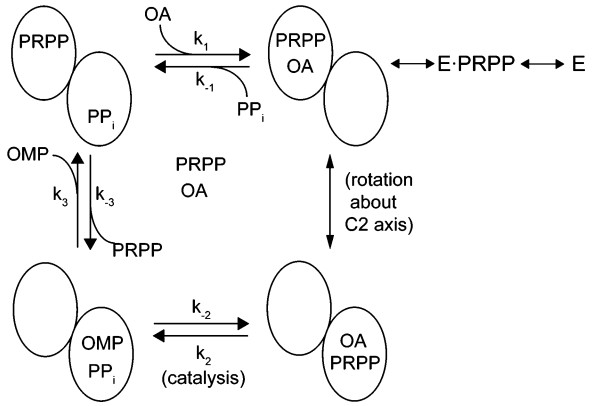

microscopic rate constants were extracted along with the K_m values from the rate equation in the form $v = V[A][B]/(K_{mA}[B] + K_{mB}[A] + [A][B])$.

The first-order rate constants (k_3 and k_{-1} for the quasi-classical Theorell−Chance models and k_2 and k_{-2} for the "double Theorell−Chance" model) are in reasonable agreement (Table 1) with the specific activities of the enzyme in the forward and reverse directions (39 and 25 s^{-1}, respectively) determined in our work. Those values correspond to the catalytic events in the "double Theorell−Chance" mechanism. Additionally, in the case of the "double Theorell−Chance" model, it is seen that the four second-order rate constants (k_1, k_{-1}, k_3, and k_{-3}) are all quite similar (approximately 10^6 M^{-1} s^{-1}) and not more than 1 or 2 orders of magnitude below the diffusion-controlled limit. Thus, if this kinetic mechanism were correct, it would appear that OPRTase maintains roughly equal concentrations of each intermediate species. The equilibrium constant most removed from unity is k_3/k_{-3}, which is 0.24, qualitatively consistent with our finding that OMP is bound more tightly to the apoenzyme than is PRPP. Indeed, if the physiological [OA] and [PRPP] were each approximately at their K_m values, a reasonable assumption (*28*), then all three steps in the biosynthetic cycle (Scheme 4) would be occurring at about the same rate and the three forms of the enzyme would have roughly equal concentrations. It is noteworthy that the calculated rate for binding of OMP at its point in the catalytic cycle (1.3 × 10^7 M^{-1} s^{-1}) is very close to the experimental value for the addition of OMP to apo OPRTase (3.6 × 10^7 M^{-1} s^{-1}).

Finally, one can also obtain the inverse of the modified general rate equations to predict the patterns of product inhibition. Considering PRPP as an inhibitor in the "reverse" reaction, if one varies, for example, [OMP] at a fixed [PP_i], where $[OA]_o = 0$, one obtains the following equation:

$$\frac{[E]_t}{v} = \frac{1 + k_2 + k_{-2}}{k_{-1}k_{-2}[PP_i]} + \left(\frac{1}{[OMP]}\right)\frac{k_{-2} + [PRPP](k_{-2}k_3 + k_{-1}k_3[PP_i])}{k_{-1}k_{-2}k_{-3}} \quad (8)$$

which reveals that the intercept of a double-reciprocal plot will remain constant, while the slope increases with the [PRPP] as one would expect for competitive inhibition with a Theorell−Chance mechanism, where a subtrate/product pair enter/leave co-temporally. Likewise, for the proposed "double Theorell−Chance" mechanism, it is easily shown that the competitive inhibition patterns hold for OMP versus PRPP, OA versus PP_i, and PP_i versus OA and that the same is true for the noncompetitive patterns for PRPP versus PP_i, etc. Thus, we can find nothing in the entire body of kinetics and binding studies that is inconsistent with the model proposed.

It is possible that yeast OPRTase may have evolved to employ alternating site catalysis to keep the free energy of intermediate enzyme states equal and, more importantly, to use the binding energy of an incoming reactant to aid in the dissociation of its companion, most likely accompanied by a conformational change in the enzyme. Indeed, hypoxanthine-guanine PRTase, another dimeric type-I PRTase (*29*), has been observed to exist with simultaneous "open" and "closed" subunits in the crystal structures with bound PRPP and the purine analogue HPP in similar fashion to the OPRTase from *E. coli* with two sulfate ions bound (*7*). The precise details of how some half-of-sites proteins that employ cooperative conformational changes have come to light recently (for example, refs *30*−*33*), and it appears that yeast

OPRTase is a member of this group. It is interesting to note that the original Theorell−Chance enzyme, liver alcohol dehydrogenase (*34*), was later shown to follow a form of half-sites reactivity (*35*), and it is tempting to speculate that the apparent simultaneous binding and release of alcohol/aldehyde, which otherwise seem hard to explain, occur across the subunits as we propose for OPRTase and its substrates. Such schemes were dubbed "flip-flop" mechanisms 33 years ago (*36*). An important feature of such enzymes is that they may demonstrate Michaelis−Menten kinetics (*36*, *37*) and thus potentially escape notice. Indeed, we suggest that such mechanisms may well turn out to be quite common.

Future experiments will focus on testing the validity of the "double Theorell−Chance" mechanism. A 2.6 Å crystal structure of *Saccharomyces* OPRTase has recently been obtained and, with further refinement and with ligands included, should aid in the investigation of how this intriguing enzyme accomplishes the synthesis of OMP.

SUMMARY

Yeast OPRTase exhibits strict half-of-sites reactivity, as evidenced by the formation of 1:1 complexes with either OMP or PRPP. These findings suggest that OPRTase does not follow a quasi-classical Theorell−Chance mechanism of the types shown in Schemes 2 or 3, but rather, all data are consistent with a novel variation in which there are two effectively simultaneous displacements of products across the subunits per catalytic cycle, with the binding of substrates to one subunit of the dimer facilitating the release from the adjacent subunit, yielding kinetic results previously attributed only to classical ping-pong bi-bi enzymes.

ACKNOWLEDGMENT

The authors thank Dr. Steve Short (GlaxoSmithKline) for providing pure yeast ODCase, Rachael Relph, B. Chris Hoefler, and Katherine Stoll for help with preliminary studies, and Prof. Paul D. Boyer for helpful insights.

SUPPORTING INFORMATION AVAILABLE

Figure S1, the relative retention times of apo OPRTase and OMP·OPRTase along with standards upon analytical gel-filtration HPLC to demonstrate that the OMP·OPRTase complex involves the dimeric form of the enzyme; Figure S2, a series of UV spectra that demonstrates the conversion of OMP·OPRTase to the apoenzyme and UMP catalyzed by ODCase. This material is available free of charge via the Internet at http://pubs.acs.org.

REFERENCES

1. Smith, J. L. (1999) Forming and inhibiting PRTase active sites, *Nat. Struct. Biol. 6*, 502−504.
2. Krahn, J. M., Kim, J. H., Burns, M. R., Parry, R. J., Zalkin, H., and Smith, J. L. (1997) Coupled formation of an amidotransferase interdomain ammonia channel and a phosphoribosyltransferase active site, *Biochemistry 36*, 11061−11068.
3. Scapin, G., Grubmeyer, C., and Sacchettini, J. C. (1994) Crystal structure of orotate phosphoribosyltransferase, *Biochemistry 33*, 1287−1294.
4. Scapin, G., Ozturk, D. H., Grubmeyer, C., and Sacchettini, J. C. (1995) The crystal structure of the orotate phosphoribosyltransferase complexed with orotate and α-D-5-phosphoribosyl-1-pyrophosphate, *Biochemistry 33*, 1287−1294.
5. Wang, G. P., Lundegard, C., Jensen, K. F., and Grubmeyer, C. (1999) Kinetic mechanism of OMP synthase: A slow physical step following group transfer limits catalytic rate, *Biochemistry 38*, 275−283.
6. Wang, G. P., Cahill, S. M., Liu, X., Girvin, M. E., and Grubmeyer, C. (1999) Motional dynamics of the catalytic loop in OMP synthase, *Biochemistry 38*, 284−295.
7. Henriksen, A., Aghajari, N., Jensen, K. F., and Gajhede, M. (1996) A flexible loop at the dimer interface is a part of the active site of the adjacent monomer of *Escherichia coli* orotate phosphoribosyltransferase, *Biochemistry 35*, 3803−3809.
8. Pearson, W. R., and Lipman, D. J. (1988) Improved tools for biological sequence comparison, *Proc. Natl. Acad. Sci. U.S.A. 85*, 2444−2448.
9. Victor, J., Greenberg, L. B., and Sloan, D. L. (1979) Studies of the kinetic mechanism of orotate phosphoribosyltransferase from yeast, *J. Biol. Chem. 254*, 2647−2655.
10. Goitein, R. K., Chelsky, D., and Parsons, S. M. (1978) Primary ^{14}C and α secondary ^{3}H substrate kinetic isotope effects for some phosphoribosyltransferases, *J. Biol. Chem. 253*, 2963−2971.
11. Witte, J. F., Tsou, R., and McClard, R. W. (1999) Cloning, overproduction, and purification of native and mutant recombinant yeast orotate phosphoribosyltransferase and the demonstration from magnetization inversion transfer that a proposed oxocarbocation does not have a kinetic lifetime, *Arch. Biochem. Biophys. 361*, 106−112.
12. Bhatia, M. B., Vinitsky, A., and Grubmeyer, C. (1990) Kinetic mechanism of orotate phosphoribosyltransferase from *Salmonella typhimurium*, *Biochemistry 29*, 10480−10487.
13. Cleland, W. W. (1977) Determining the chemical mechanisms of enzyme-catalyzed reactions by kinetic studies, *Adv. Enzymol. 45*, 273−387.
14. Fromm, H. J. (1975) *Initial Rate Enzyme Kinetics*, Springer-Verlag, New York.
15. Levine, H. L., Brody, R. S., and Westheimer, F. H. (1980) Inhibition of orotidine-5′-phosphate decarboxylase by 1-(5′-phospho-β-D-ribofuranosyl)barbituric acid, 6-azauridine 5′-phosphate, and uridine 5′-phosphate, *Biochemistry 19*, 4993−4999.
16. Ueda, T., Yamamoto, M., Yamane, A., Imazawa, M., and Inoue, H. (1978) Nucleosides and nucleotides. 13. Conversion of uridine nucleotides to 6-cyano derivatives−Synthesis of orotidylic acid, *J. Carbohydr., Nucleosides, Nucleotides 5*, 261−271.
17. Rishavy, M. A., and Cleland, W. W. (2000) Determination of the mechanism of orotidine 5′-phosphate decarboxylase by isotope effects, *Biochemistry 39*, 4569−4574.
18. Rawls, J. M. (1978) Enzymatic synthesis of [6-^{14}C] orotidine 5′-monophosphate and its use in the assay of orotate phosphoribosyltransferase and orotidylate decarboxylase, *Anal. Biochem. 86*, 107−117.
19. Ames, B. M. (1966) Assay of inorganic phosphate, total phosphate and phosphatases, *Methods Enzymol. 8*, 115−118.
20. Eftink, M. R. (1997) Fluorescence methods for studying equilibrium macromolecule-ligand interactions, *Methods Enzymol. 278*, 221−257.
21. Robinson, G., Kuchel, P. W., Chapman, B. E., Doddrell, D. M., and Irving, M. G. (1985) A simple procedure for selective inversion of NMR resonances for spin transfer enzyme kinetic measurements, *J. Magn. Reson. 63*, 314−319.
22. Meyer, R. A., Kushmerick, M. J., and Brown, T. R. (1982) Application of ^{31}P NMR spectroscopy to the study of striated muscle metabolism, *Am. J. Physiol. 242* (*Cell Physiol. 11*), C1−C11.
23. Umezu, K., Amaya, T., Yoshimoto, A., and Tomita, K. (1971) Purification and properties of orotidine-5′-phosphate pyropyhosphorylase and orotidine-5′-phosphate decarboxylase from baker's yeast, *J. Biochem. 70*, 249−262.
24. Sugano, T., Kitagawa, T., Tsuda, Y., Shibutani, T., and Kubo, K. (1972) Heats and entropies of reaction of alkaline-earth metal ions with pyrophosphate and triphosphate ions, *Nippon Kagaku Kaishi 4*, 734−739.
25. Kline, P. C., and Schramm, V. L. (1992) Purine nucleoside phosphorylase. Inosine hydrolysis, tight binding of the hypoxanthine intermediate, and third-the-sites reactivity, *Biochemistry 31*, 5964−5973.
26. Boyer, P. D. (1997) The ATP synthase−A splendid molecular machine, *Annu. Rev. Biochem. 66*, 717−749.
27. King, E. L., and Altman, C. (1956) A schematic method of deriving the rate laws for enzyme-catalyzed reactions, *J. Phys. Chem. 60*, 1375−1378.

28. Atkinson, D. E. (1977) *Cellular Energy Metabolism and Its Regulation*, Academic Press, San Diego, CA, p 116 *ff*.
29. Focia, P. J., Craig, S. P., III, and Eakin, A. E. (1998) Approaching the transition state in the crystal structure of a phosphoribosyltransferase, *Biochemistry 37*, 17120−17127.
30. Biemann, H.-P., and Koshland, D. E., Jr. (1994) Aspartate receptors of *Escherichia coli* and *Salmonella typhimurium* bind ligand with negative and half-of-the-sites cooperativity, *Biochemistry 33*, 629−634.
31. Anderson, A. C., O'Neil, R. H., DeLano, W. L., and Stroud, R. M. (1999) The structural mechanism for half-the-sites reactivity in an enzyme, thymidylate synthase, involves a relay of changes between subunits, *Biochemistry 38*, 13829−13836.
32. Nichols, C. E., Dhaliwal, B., Lockyer, M., Hawkins, A. R., and Stammers, D. K. (2004) High-resolution structures reveal details of domain closure and "half-of-sites" reactivity in *Escherichia coli* aspartate β-semialdehyde dehydrogenase, *J. Mol. Biol. 341*, 797−806.
33. Frank, R. A. W., Titman, C. M., Pratap, J. V., Luisi, B. F., and Perham, R. N. (2004) A molecular switch and proton wire synchronize the active sites in thiamine enzymes, *Science 306*, 872−876.
34. Theorell, H., and Chance, C. B. L. (1951) Studies on liver alcohol dehydrogenase II. The kinetics of the compound of horse liver alcohol dehydrogenase and reduced diphosphopyridine nucleotide, *Acta Chem. Scand. 5*, 1127−1144.
35. Bernhard, S. A., Dunn, M. F., Luisi, P. L., and Schack, P. (1970) Mechanistic studies on equine liver alcohol dehydrogenase. I. The stoichiometry relationship of the coenzyme binding sites to the catalytic sites active in the reduction of aromatic aldehydes in the transient state, *Biochemistry 9*, 185−192.
36. Lazdunski, M. (1972) Flip-flop mechanisms and half-site enzymes, *Curr. Top. Cell. Regul. 6*, 267−310.
37. Seydoux, F., Malhotra, O. P., and Bernhard, S. A. (1974) Half-site reactivity, *CRC Crit. Rev. Biochem. 2*, 227−257.

BI051650O